

Electroreflectance and surface photovoltage spectroscopies of semiconductor structures using an indium–tin–oxide-coated glass electrode in soft contact mode

Shouvik Datta^{a)}

Department of Condensed Matter Physics and Materials Sciences, Tata Institute of Fundamental Research, Homi Bhabha Road, Mumbai-400 005, India

Sandip Ghosh

Paul Drude Institut für Festkörperelektronik, Hausvogteiplatz 5-7, D-10117, Berlin, Germany

B. M. Arora

Department of Condensed Matter Physics and Materials Sciences, Tata Institute of Fundamental Research, Homi Bhabha Road, Mumbai-400 005, India

(Received 27 June 2000; accepted for publication 17 October 2000)

Measurements of electroreflectance and surface photovoltage spectroscopy of semiconductor structures are described using a transparent indium–tin–oxide-coated glass electrode in soft contact mode on the semiconductor surface. This improvisation (simplification) reduces the magnitude of the ac modulation voltage necessary for the electroreflectance measurement to less than a volt from about a kV ($\sim 10^3$ V) as required in the conventional contactless setup. This soft contact mode also enhances the sensitivity of the surface photovoltage signal by three orders of magnitude. We also formulate an analytical criterion to extract the transition energies of a quantum well from the surface photovoltage spectrum. © 2001 American Institute of Physics. [DOI: 10.1063/1.1332114]

I. INTRODUCTION

Characterization of as-grown semiconductor structures for optoelectronic and other device applications is of considerable interest. Photorefectance¹ (PR) spectroscopy is widely used for nondestructive testing of band gaps, layer composition, etc. An alternative electromodulation technique, contactless electroreflectance (CER),² has also been used by many workers with the advantage that the sample can be cooled and measurement can be done without unwanted photoluminescence (PL),³ particularly at low temperatures. This low-temperature PL background problem of PR can also be remedied by dual-chopping PR,⁴ where both pump and probe beams are chopped at different frequencies and the reflected signal is detected at the sum frequency. While CER has some advantages, its use is limited because of the need of a high-voltage source for modulating the electric field. Recently, surface photovoltage spectroscopy⁵ has also become widely used for characterizing bulk and quantum structures of semiconductors. In this article we will discuss some novel modifications of the conventional setup of both electroreflectance (ER) and surface photovoltage (SPV) spectroscopies and show that these modified techniques are spectroscopically equivalent to the conventional measurement procedures. Moreover, they also have some additional advantages and simplicity. However, use of SPV spectroscopy is relatively limited because of some analytic difficulties in extracting the transition-energy values from the SPV

spectrum. Here, we will also try to formulate an analytical criterion for extracting the transition energies of a quantum well (QW) from the SPV spectrum.

II. SOFT CONTACT ELECTROREFLECTANCE SPECTROSCOPY

In general, ER^{6–9} spectroscopy can be broadly categorized in (1) longitudinal modes, and (2) transverse modes of electromodulation schemes. In the longitudinal methods, where the modulation voltage is applied across the front and back surfaces of the sample, electromodulation can be achieved by various sample configurations like (1) liquid electrolyte mode,^{10,11} (2) metal–insulator–semiconductor (MIS) structures,^{12,13} (3) Schottky barrier methods,^{14,15} (4) $p-i-n$ structure,^{16,17} as well as (5) the contactless method or CER.² The liquid electrolyte method is simple to implement but can be used only over a limited temperature range around room temperature (~ 300 – 150 K) and offers less control of the space-charge field owing to chemical passivation or dissolution effects. The rest of the above methods can also be used at low temperatures, albeit with other limitations. The MIS method requires careful sample preparation or deposition of some oxide layer on the sample. Schottky barrier configuration requires smaller voltage to operate; however, it needs metal electrodes to be deposited on the sample surface, which by itself is a destructive technique. The $p-i-n$ structure can be used on specially fabricated samples and produces a constant electric field as opposed to a position-dependent field of other longitudinal ER modes. In the transverse mode^{18–20} two metal electrodes are evaporated on the front surface of the sample and electromodulation is pro-

^{a)}Electronic mail: shouvik@tiffr.res.in

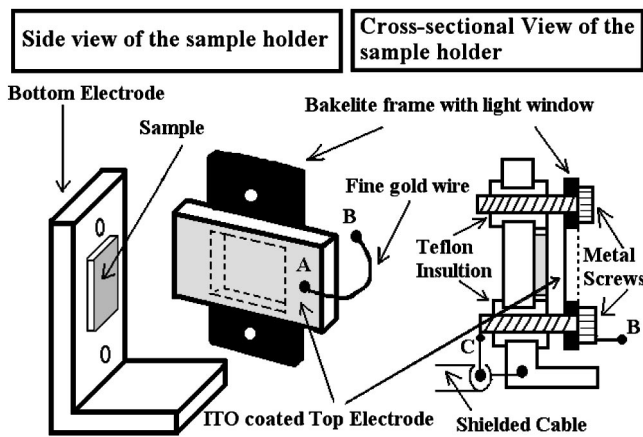


FIG. 1. Schematic diagram of the sample holder used in both ER and SPV measurements.

duced by applying high voltage (\sim kV) across the thin (\sim 1 mm) gap between the electrodes. However, this technique can only be used on materials with resistivities greater than $\sim 10^8 \Omega \text{ cm}$. Among all these various ways of ER spectroscopy, the most recent and most commonly used ER spectroscopy is CER.² In CER, a transparent indium–tin–oxide (ITO) electrode separated from the sample surface by a fraction of a millimeter is generally used for the application of modulation voltage as well as the window for the incident and reflected light. Although CER is a nondestructive technique and requires no sample preparation, it also suffers from the drawback of using high voltage (\sim kV) for electric-field modulation. In an effort to reduce the modulation voltage, we make the ITO electrode softly touch the semiconductor surface. This “soft touch” means the spacing between the sample surface and the ITO-coated electrode is reduced until Newton’s rings become visible, so that the capacitive impedance of the whole two electrode assembly including the sample (i.e., front ITO electrode, sample, and back electrode) is limited by the sample itself, as will be explained below. We have found that in this way the modulation voltage can be reduced considerably to less than a volt, and in some cases to few tens of mV.

Figure 1 shows schematically the construction of the sample holder. It consists of a grounded L-shaped copper back electrode on which the sample is mounted. The base of L-shaped plate is clamped on the cryostat cold head/finger. The top electrode is an ITO-coated glass slide. The uncoated side of the glass is attached on a Bakelite frame with a rectangular window. Two metal screws join the top and bottom electrode assembly together such that the ITO-coated electrode softly touches the sample surface as mentioned above. We call this soft contact electroreflectance (SCER). A fine gold wire is electrically connected to the ITO-coated surface (point A in Fig. 1) on one side and to the metal screw holder on the other side (point B in Fig. 1) of the Bakelite plate. The screws are electrically insulated from the back electrode with threaded Teflon rings embedded inside both of the holes in the back electrode which is kept at ground potential. A shielded cable is connected between the other end of the screw (point C in Fig. 1) and the back electrode. In the case

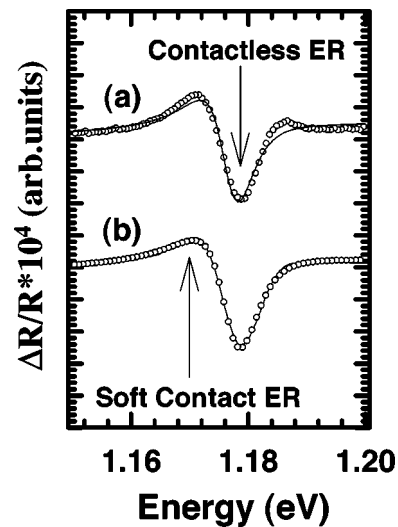


FIG. 2. (a) CER spectrum of the e_1-hh_1 transition, (b) SCER spectrum of the e_1-hh_1 transition of the GaAs/In_{0.26}Ga_{0.74}As/GaAs single QW structure. Both spectra are fitted with the Aspnes line-shape function with $m=2$, as shown by continuous lines. Respective spectra are vertically displaced and plotted separately.

of ER, we apply the modulating ac voltage between these electrodes. A 150 W quartz–tungsten–halogen lamp and monochromator arrangement is used as a light source. Light output centered at some wavelength is focused on the sample with a lens and mirror arrangement. The window in the Bakelite holder and the transparent ITO-coated glass allow the probe light to be incident (at near-normal incidence) on the sample, and also allow the reflected light from the sample to go out. The reflected light is collected with a Ge photovoltaic detector. Proper-order-sorting filters are used in front of the Ge detector to block any unwanted light. Current from the detector is transformed into a voltage signal by a current-to-voltage converter and fed into a SRS830 lock-in amplifier. The experimental bandpass ($\Delta\lambda$) of the monochromator is kept at $\sim 32 \text{ \AA}$. The change in the reflectivity [$\Delta R(\lambda)$] is measured with the lock-in amplifier, in phase with the applied ac. The dc part of the signal [$R(\lambda)$] is separated and fed to the analog-to-digital port of the same lock-in amplifier. After the measurements, we numerically calculate $\Delta R(\lambda)/R(\lambda)$ vs λ and get the ER spectrum.

Figure 2 shows two ER spectra of a sample containing a 100- \AA -thick strained In_{0.26}Ga_{0.74}As single quantum well in the GaAs/In_{0.26}Ga_{0.74}As/GaAs structure. Dotted curve (a) in Fig. 2 is the ER spectrum of the e_1-hh_1 transition as obtained by the conventional contactless mode (CER) and curve (b) in Fig. 2 is the ER spectrum as obtained in the new SCER mode under similar experimental settings. The only difference between the two is the amplitude of the ac voltage applied during the measurement. In the case of CER, we apply an ac amplitude of $\sim 1.25 \text{ kV}$ for electromodulation, while in the SCER configuration we apply only 0.5 V ac amplitude. The continuous curves in Fig. 2 are fitted using the Aspnes⁹

$$\frac{\Delta R}{R} = \sum_{j=1}^n \text{Re}[a_j \exp(i\theta_j) / (E - E_{0j} + i\Gamma_j)^m], \quad i = \sqrt{-1}, \quad (1)$$

first-derivative line-shape function ($m=2$, assuming Lorentzian broadening) to the experimental data. The e_1-hh_1 transition-energy values, as obtained from the line-shape fitting from the two curves are, respectively, $E_0=1.1768$ eV in contactless mode and $E_0=1.1774$ eV in SCER (with experimental resolution $\Delta E\sim 3$ meV). The fitted values of the broadening parameter (Γ) are also nearly the same within experimental error (5.69 meV in the contactless mode and 6.07 meV in the soft contact mode). This shows that SCER is as reliable a spectroscopic technique as conventional CER and it has all the experimental advantages of CER as mentioned above. Moreover, SCER has added advantages because it does not require a high-voltage source, which (i) simplifies the electronics, (ii) reduces experimental hazards, (iii) reduces the chance of damage to the sample from accidental electrical discharge, and (iv) avoids the possibility of spurious pickup from the high-voltage ac unit into the weak modulated reflectivity signal.

To understand the reasons behind this reduction in the applied voltage, we consider an ideal case where the top ITO electrode and sample surface are assumed to be parallel to each other. We note that for an air-gap separation (d) of the sample and the ITO electrode of ~ 0.3 mm, the capacitance of the air gap is $C_{\text{air}}\sim 1.48\times 10^{-13}$ F for $\epsilon_{\text{air}}=8.85\times 10^{-14}$ F/cm and area 0.05 cm². On the other hand, for a 10^{16} /cm³-doped n -GaAs sample with depletion depth $W=0.3$ μm , static dielectric constant of ~ 12.9 , the capacitance of the sample is $C_{\text{sem}}\sim 1.9\times 10^{-9}$ F. Assuming the C_{air} and C_{sem} are in series, we see that in the CER mode, most of the applied 1.25 kV ac amplitude is actually dropped across the air gap and only ~ 0.1 V is applied across the sample, which is sufficient to modulate the reflectivity spectrum. In the SCER mode, the impedance of the air-gap capacitor for a gap of, say, 100 \AA , becomes comparable to the impedance of the above sample. As a result, half of the applied voltage between the ITO and the ground electrode will drop across the sample. If the gap is made even smaller, then the fraction of the applied voltage dropping across the sample will be correspondingly larger. So, we can easily modulate the reflectivity spectrum by applying a low modulating voltage in the SCER. In reality, the sample surface and the surface of the top electrode will generally not be absolutely parallel or flat. In that case, the top electrode will touch the sample surface at some places and form a wedge structure such that a large number of small air gas are present between the sample and the top electrode. In this case, the required modulation voltage will depend on the relative magnitudes of C_{sem} and $C_{\text{air}}^{\text{eq}}$, where $C_{\text{air}}^{\text{eq}}$ is the corresponding equivalent capacitance of the small air gaps in parallel at the spot where the probe light beam falls on the sample. Thus, even if $C_{\text{air}}^{\text{eq}}$ is smaller than C_{sem} by an order of magnitude, we need to apply only 1 V to get ~ 0.1 V drop across the sample, which is sufficient to obtain the ER signal.

Figure 3 shows a plot of the modulated reflectance (ΔR) for a e_1-hh_1 transition in the SCER experiment on another sample in which two 70- \AA -thick strained $\text{In}_{0.26}\text{Ga}_{0.74}\text{As}$ QWs separated by 150 \AA GaAs are sandwiched between p - and n -type GaAs. ΔR varies with the modulation potential, and in this case, we are able to

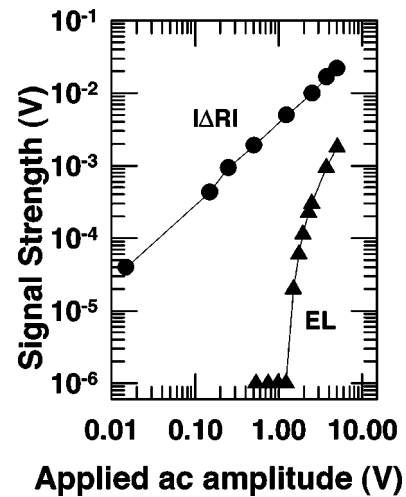


FIG. 3. Comparison of the maximum (ΔR) signal of the e_1-hh_1 transition from SCER and the EL background at various ac amplitudes. EL background vanishes below ~ 1.25 V.

reduce the applied ac amplitude to ~ 15 mV and still get a good ER line shape. At this point, we would like to comment on the upper limit of the ac amplitude that can be applied during a SCER measurement. Applying a large modulating voltage may heat up the sample or produce an unwanted electroluminescence (EL)²¹ signal, which can distort the ER line shape. We have measured the EL background of the above sample under various applied ac voltages with the light from the monochromator blocked. As shown in Fig. 3, reduction in the applied ac voltage reduces this EL background sharply. For this particular sample, we see that below ~ 1.25 V ac amplitude the EL background vanishes totally and merges with the noise level. Therefore, for this sample it is preferable to apply ac volts below this value while doing the SCER measurements. Therefore, a preliminary measurement of the EL background is performed for each sample and the maximum ac voltage which is allowed without any unwanted EL background contribution is determined before the actual SCER measurement. Alternatively, in case the sample does not emit EL, the series current can be monitored to avoid excessive heating of the sample. In our measurements, the series current is always limited to less than about 10 μA .

Another contribution to the upper limit of the applied ac value will come from a well-known standard criterion. For transitions in bulk materials, the third-derivative Lorentzian broadened Aspnes line shape in the low-field limit⁹ can only be used in the case of $\Delta R/R\leq 10^{-3}$. So one should experimentally determine these two limits for each sample before recording a SCER spectrum for further analysis.

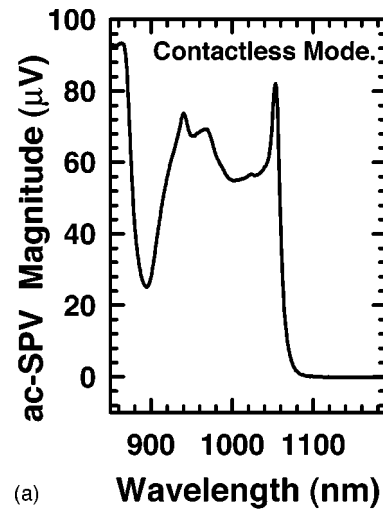
III. SOFT CONTACT SURFACE PHOTOVOLTAGE SPECTROSCOPY

Surface photovoltage spectroscopy (SPS) is a well-known technique to map the electronic structure of bulk semiconductors near the band edge as well as at subband-gap energies. In surface photovoltage,²²⁻²⁹ we measure the change in surface potential due to optically excited electron-hole pair generation under periodic illumination and subse-

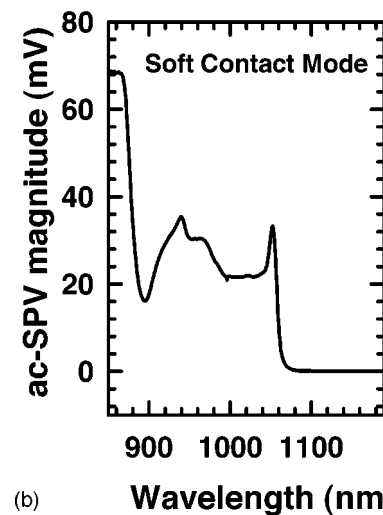
quent carrier redistribution and/or capture in the surface states. Recently, SPV has emerged as a powerful technique⁵ to study surface states,^{30–35} heterojunctions,^{36,37} quantum wells,^{38–40} and other nanostructures.^{41–43} Various techniques like the Kelvin probe method,^{44–46} MIS structure,^{47–51} direct-contact measurements like the electrolyte method,⁵² depositing a semitransparent metallic contact,^{53–57} or depositing a transparent conductor^{58–60} on the sample have been used to measure the SPV. The Kelvin probe technique uses a null capacitive method of measuring the SPV (\approx contact potential difference) by applying external dc bias. Although it has been widely used, the Kelvin probe method suffers from noise-related problems, as a result of the residual electrostatic pickup by the Kelvin capacitor as well as the stray capacitances, which necessitates the use of careful electrical shielding. SPV measurements using a fabricated MIS structure on a semiconductor sample are also useful, but the technique requires special sample preparation. Alternatively, an insulating spacer or air/vacuum gap can be used between the sample and the front electrode. But, this reduces the capacitive coupling of the electrodes with the sample. As a result, the measured SPV is much less than the intrinsic SPV generated within the sample. The electrolyte method suffers from surface passivation and dissolution effects as well as a limited temperature range of operation. All the other methods of depositing a semitransparent metal or transparent conducting film on the sample are useful, but these are obviously destructive techniques.

The same soft contact mode arrangement of the two-electrode assembly including the sample (as described in the previous section and in Fig. 1) is also useful for sensitive nondestructive measurements of surface photovoltage spectra. We call this method the soft contact surface photovoltage (SCSPV) experiment. For SCSPV measurements, we periodically chop the light incident on the sample and measure the photovoltage produced due to separation of photogenerated carriers under surface electric fields. Instead of applying ac voltage from outside as in SCER, we pick up the above-mentioned ac SCSPV signal with the same set of electrodes and leads. Finally, by recording the SPV signal $S(\lambda)$ vs λ in phase with the chopped light as the wavelength (λ) of the incident light is varied, we get the SCSPV spectrum. In this case, we use appropriate order-sorting filters just after the monochromator to prevent unwanted light from falling on the sample.

In Fig. 4 we plot the SPV spectra of the QW sample used for the CER/SCER measurements, as shown in Fig. 2. Figure 4(a) is the SPV spectrum as measured in the usual contactless mode and Fig. 4(b) is the SCSPV spectrum. The main features corresponding to the band edge of GaAs and the $\text{In}_{0.26}\text{Ga}_{0.74}\text{As}$ single QW are reproduced in both experiments. For further comparison of the transition energies we calculate the numerical derivative spectrum, $d[E \times \text{SPV}(E)/dE]$ vs E , where E is the incident energy, and fit the Aspnes line-shape function [Eq. (1)] with $m=2$. This procedure can be justified as follows. We assume that the SPV magnitude can be written as the open-circuit photovoltage (V_{OC}) such that⁶¹



(a)



(b)

FIG. 4. (a) SPV spectrum in the contactless mode, (b) SCSPV spectrum of the $\text{GaAs}/\text{In}_{0.26}\text{Ga}_{0.74}\text{As}/\text{GaAs}$ single QW structure.

$$\text{SPV} \cong V_{OC} = \frac{kT}{q} \ln \left(1 + \frac{I_{ph}}{I_0} \right), \quad (2)$$

where I_{ph} is the short-circuit photocurrent, I_0 is dark current, k is the Boltzmann constant, q is electric charge, and T is sample temperature. For a thin absorbing layer of thickness t (e.g., 100 Å QW), $\alpha t \ll 1$, where α is the absorption coefficient. In the case of selective photogeneration only within the QW (E_g of the well $< h\nu < E_g$ of the barrier), photo current density I_{photo} can be written as

$$\begin{aligned} I_{photo} &= \left(\frac{A \eta q \Phi_0 (1-R)}{h\nu} \right) \times [1 - \exp(-\alpha t)] \\ &\approx \frac{A \eta q \Phi_0 (1-R)}{h\nu} \times (\alpha t), \end{aligned} \quad (3)$$

where $\Phi(x)$ is the light intensity at a distance x within the sample such that $\Phi(x) = \Phi_0 \exp(-\alpha x)$, Φ_0 being the incident light intensity and R is the reflectivity, η is the quantum efficiency, A is the illuminated area of the sample, and $h\nu$ is the incident photon energy. In the region of the QW spectrum, the measured spectral response of the excitation light

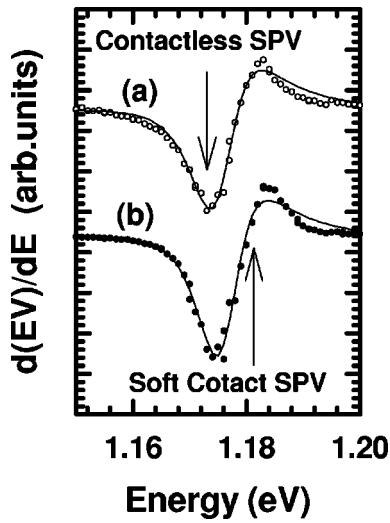


FIG. 5. (a) SPV spectrum of the e_1-hh_1 transition in the contactless mode, (b) SCSPV spectrum of the e_1-hh_1 transition of the GaAs/In_{0.26}Ga_{0.74}As/GaAs single QW structure. Both spectra are fitted with the Aspnes line-shape function with $m=2$, as shown by continuous lines. Respective spectra are vertically displaced and plotted separately.

from the lamp and monochromator combination is found to be nearly independent of wavelength, thus requiring no further correction for excitation intensity normalization.⁴¹ By suitably choosing Φ_0 , we can arrange the equation such that $I_{ph} \ll I_0$. Then from Eq. (2), we find that V_{OC} is proportional to $(kT/q)(I_{ph}/I_0)$. Using this with Eq. (3), we see that

$$SPV \propto \frac{\alpha}{h\nu}. \quad (4)$$

Assuming that the variation in R is small compared to the variation in α near the optical transition, we find that $[(h\nu) \times SPV(h\nu)]$ is proportional to the absorption coefficient $\alpha(h\nu)$. We see from Eq. (4) that the numerically differentiated quantity $d[h\nu \times SPV(h\nu)]/d(h\nu)$ actually scales as $d\alpha/d(h\nu)$. Using elementary calculus and the facts that $\alpha = 2\pi\nu\epsilon_2(\omega)/nc$, $\epsilon = n^2$ and $\epsilon(\nu) = \epsilon_1(\nu) + i\epsilon_2(\nu)$, one can derive⁶² the differential relation $d\alpha$ in terms of $\Delta\epsilon_1$ and $\Delta\epsilon_2$ as

$$d\alpha(\nu) = \gamma(\nu)\Delta\epsilon_1(\nu) + \delta(\nu)\Delta\epsilon_2(\nu), \quad (5)$$

where $\gamma(\nu)$ and $\delta(\nu)$ are similar to Seraphin coefficients used in the modulated reflectance spectroscopy. The differential relation given in Eq. (5) is generally valid and the exact functional form of $\Delta\epsilon_1$ and $\Delta\epsilon_2$ are different depending on the physical situation. When we calculate the numerically differentiated quantity $d[h\nu \times SPV(h\nu)]/d(h\nu)$ or $d\alpha/d(h\nu)$, then these $\Delta\epsilon_1$ and $\Delta\epsilon_2$ are respective changes of ϵ_1 and ϵ_2 at two nearby energy values. The resulting spectrum is qualitatively equivalent to a wavelength-modulated⁶³ absorption spectrum. It is known⁶⁴ that the spectral features of the wavelength-modulation spectrum can be represented by first-derivative line-shape function. Therefore, with this analogy, we use the Aspnes first-derivative line-shape function having $m=2$ to fit the numerical $d(E \times SPV)/dE$ spectrum of SPV of the e_1-hh_1 transition.

Figure 5 shows the numerically differentiated SPV spectra of Fig. 4. The transition energies of the e_1-hh_1 line, as obtained by using the above-mentioned line-shape fitting (as shown by the continuous lines in Fig. 5, are $E_0 = 1.1757$ eV and $E_0 = 1.1764$ eV (with experimental resolution $\Delta E \sim 3$ meV) for contactless and soft contact modes, respectively. The broadening parameters are $\Gamma = 7.26$ meV and $\Gamma = 7.02$ meV for contactless and SCSPV modes, respectively. Within experimental accuracy, the spectroscopic signatures of the e_1-hh_1 transition energy are similar in both of these experimental methods of SPV. These transition energy values are also comparable to the values obtained above from the ER experiments on the same sample. Although agreement between the transition energies is fairly good, there still remains some questions regarding the overall shape of the SPV spectrum near the QW transitions. From Fig. 4, it is seen that in the SCSPV the ratio of the SPV magnitude for energies above the band edge of GaAs, the SPV magnitude of the QW transition is larger than the corresponding ratio in the contactless model. Further investigation is on going to explain this result, which is also seen in other samples.

Next, we shall briefly comment on the validity of the above line-shape fitting on the SPV spectrum of bulk samples. As earlier, Φ_0 should be small for $SPV \ll kT/q$. Furthermore, unless $\alpha L \ll 1$, where L is the minority-carrier diffusion length, the expression for the bulk SPV is not^{5,27} directly proportional to α , unlike in the case of QW SPV. As a result, use of the above-fitting procedure to obtain the transition-energy values is not strictly justified for bulk materials. However, empirically we have applied the same procedure to obtain transition energies for bulk GaAs at different temperatures. The resulting values when fitted with Varshni's equation^{65,66} produce parameters⁶⁷ which are in agreement with the standard values⁶⁸ accepted in the literature. These transition-energy values for bulk GaAs also match those determined from the ER experiments. Therefore, it may be argued that the above-mentioned fitting procedure to extract the transition energies may still be a good operational technique to analyze the SPV spectra of bulk materials.

The most important aspect of SCSPV is the increase in the magnitude of the signal as compared with the SPV signal in the contactless mode. The above band-edge signal of GaAs (below 877 nm) increases by nearly three orders of magnitude in the case of the soft contact mode. This is an enormous increase in the signal strength. We understand the increase of the SPV signal in the soft contact mode in the following way. Figure 6 shows a schematic diagram of the equivalent circuit of the SPV measurement. V_s is the photovoltage signal generated within the sample. Following earlier analysis of the contactless mode described above, $Z_{air} \sim 3.4 \times 10^{11} \Omega$ and $Z_{sem} \sim 26.3 \times 10^6 \Omega$ are, respectively, the impedances of the air-gap capacitor and that of the capacitor of the depletion region of the semiconductor at the measurement frequency of ~ 20 Hz. V_{meas} is the voltage measured with the lock-in. V_{out} and V_{in} are, respectively, the output and input voltages of the unity gain buffer. R_{out} (\sim a few Ω) and R_{in} are the output and input resistance of the OP-AMP. R_{in} is ~ 500 M Ω for a maximum bias current of ~ 20 nA. We

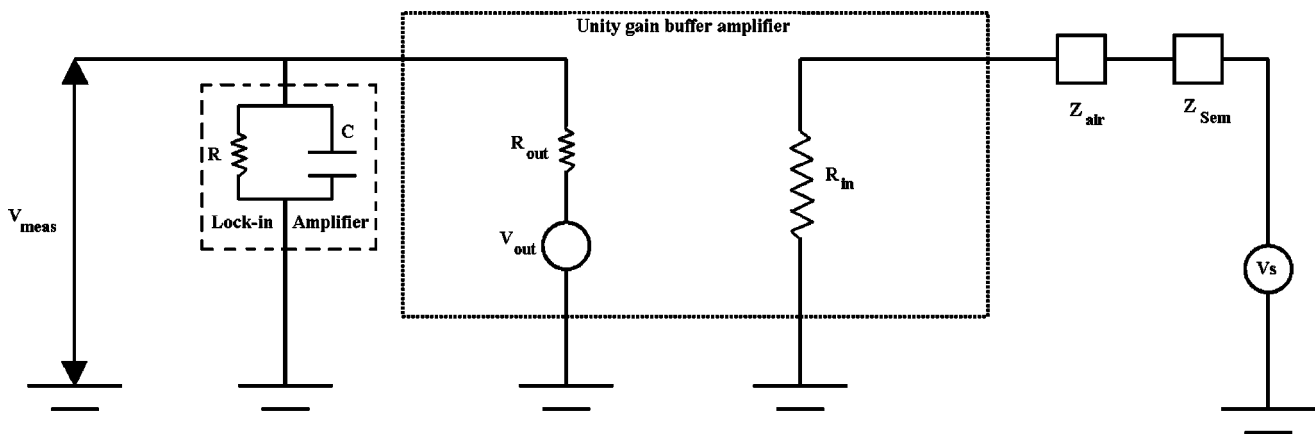


FIG. 6. Equivalent circuit diagram of the SPV setup. Z_{air} reduces drastically in the soft contact mode.

see from Fig. 6 that $V_{\text{meas}} \approx V_{\text{out}} \sim V_{\text{in}}$ as the buffer's gain is unity. So, $V_{\text{meas}} \approx V_s R_{\text{in}} / (Z_{\text{air}} + Z_{\text{sem}} + R_{\text{in}})$. If we adjust $Z_{\text{air}} \approx Z_{\text{sem}}$ in the soft contact mode, then the ratio between the measured voltage in the soft contact mode to the contactless mode is $(Z_{\text{air}} + Z_{\text{sem}} + R_{\text{in}}) / (2Z_{\text{sem}} + R_{\text{in}})$, which for the magnitudes given above is approximately $\sim 0.6 \times 10^3$. This is in agreement with the experimentally determined ratio.

One important point to be noted is the fact that I_{ph} is a function of Φ_0 . Before applying the above fitting procedure one must optimize Φ_0 such that $V_{\text{OC}} \ll kT/q$. We would also like to remark that due to the decrease in the capacitive coupling in the conventional contactless way of doing the SPV, the measured SPV magnitude may be much less than the actual SPV magnitude generated within the sample. This may create a false impression that SPV is smaller than kT , whereas in reality it may be much larger.

Due to the enhancement of the signal strength in SCSPV, we could also measure weak SPV spectra of low surface barrier materials such as p -GaAs and n -InP ($\sim \mu\text{V}$ SPV magnitude at above the band-gap photon energy of the corresponding material), which is otherwise very difficult to measure in any nondestructive fashion, due to the presence of a large dark current. Figure 7 shows the SPV spectrum of

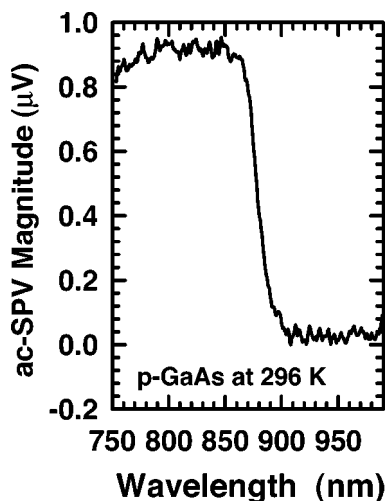


FIG. 7. SCSPV spectrum of p -GaAs. Note the sub- μV signal strength of the above band-edge SPV magnitude of p -GaAs measured at room temperature in the soft contact mode.

a bulk p -GaAs sample with doping ($\sim 5 \times 10^{16}/\text{cm}^3$). Further details of the SPV experiments on p -type GaAs and n -type InP and related aspects will be published elsewhere.⁶⁹

ACKNOWLEDGMENTS

The authors acknowledge helpful discussions with Dr. Shailendra Kumar. One of the authors (S.D.) thanks Dr. Arnab Bhattacharaya and S. S. Chandvankar for helping the authors to grow some samples, as well as V. M. Upalekar and P. B. Joshi for their help. The authors also acknowledge the generous help of Dr. S. V. Raghavan of Patent Cell, Department of Atomic Energy, Government of India and M. G. Kasbekar for helping them in patenting (Indian Patent No. 846/Mum/2000, 14 September 2000) the above novel apparatus and soft contact method for doing both SCER and SCSPV measurements.

- ¹O. J. Glembocki and B. V. Shanabrook, in *Semiconductors and Semimetals*, edited by D. G. Seiler and C. L. Littler (Academic, New York, 1992), Vol. 36, p. 221.
- ²X. Yin and F. H. Pollak, *Appl. Phys. Lett.* **59**, 2305 (1991); see, also, U.S. Patent No. 5,287,169, 15 February 1994.
- ³H. B. Bebb and E. W. Williams, in *Semiconductors and Semimetals*, edited by R. K. Willardson and A. C. Beer (Academic, New York, 1972), Vol. 8, p. 181.
- ⁴S. Ghosh and B. M. Arora, *IEEE J. Sel. Top. Quantum Electron.* **1**, 1108 (1995).
- ⁵L. Kronik and Y. Shapira, *Surf. Sci. Rep.* **37**, 1 (1999).
- ⁶D. E. Aspnes and N. Bottka, in *Semiconductors and Semimetals*, edited by R. K. Willardson and A. C. Beer (Academic, New York, 1972), Vol. 9, p. 457.
- ⁷F. H. Pollak and H. Shen, *Mater. Sci. Eng., R.* **10**, 275 (1993).
- ⁸B. O. Seraphin, in *Semiconductors and Semimetals*, edited by R. K. Willardson and A. C. Beer (Academic, New York, 1972), Vol. 9, p. 1.
- ⁹D. E. Aspnes, *Surf. Sci.* **37**, 418 (1973).
- ¹⁰K. L. Shaklee, F. H. Pollak, and M. Cardona, *Phys. Rev. Lett.* **15**, 883 (1965).
- ¹¹M. Cardona, K. L. Shaklee, and F. H. Pollak, *Phys. Rev.* **154**, 696 (1967).
- ¹²R. Ludke and W. Paul, in *II-VI Semiconductors Compounds (Proc. Int. Conf., Providence)*, edited by D. G. Thomas (Benjamin, New York, 1967), p. 123.
- ¹³J. E. Fischer, *Rev. Sci. Instrum.* **42**, 872 (1971).
- ¹⁴D. E. Aspnes, *Phys. Rev. Lett.* **28**, 913 (1972).
- ¹⁵A. A. Studna, *Rev. Sci. Instrum.* **46**, 735 (1975).
- ¹⁶O. J. Glembocki, *Mater. Res. Soc. Symp. Proc.* **160**, 631 (1990).
- ¹⁷O. J. Glembocki, *Proc. SPIE* **1286**, 2 (1990).
- ¹⁸V. Rehn and D. S. Kyser, *Phys. Rev. Lett.* **18**, 848 (1967).
- ¹⁹R. A. Forman, D. E. Aspnes, and M. Cardona, *J. Phys. Chem. Solids* **31**, 227 (1970).

- ²⁰V. Rehn, Surf. Sci. **37**, 443 (1973).
- ²¹S. Ghosh and T. J. C. Hosea, Rev. Sci. Instrum. **71**, 1911 (2000).
- ²²E. O. Johnson, Phys. Rev. **111**, 153 (1958).
- ²³A. M. Goodman, J. Appl. Phys. **32**, 2550 (1961).
- ²⁴D. R. Frankl and E. A. Ulmer, Surf. Sci. **6**, 115 (1966).
- ²⁵D. L. Lile, Surf. Sci. **34**, 337 (1973).
- ²⁶C. L. Balestra, J. Lagowski, and H. C. Gatos, Surf. Sci. **64**, 457 (1977).
- ²⁷J. Lagowski, W. Walukiewicz, M. M. G. Slusarczyk, and H. C. Gatos, J. Appl. Phys. **50**, 5059 (1979).
- ²⁸S. Kumar and S. C. Agarwal, Appl. Phys. Lett. **45**, 575 (1984).
- ²⁹W. H. Howland and S. J. Fonash, J. Electrochem. Soc. **142**, 4262 (1995).
- ³⁰M. Leibovitch, L. Kronik, E. Fefer, and Y. Shapira, Phys. Rev. B **50**, 1739 (1994).
- ³¹Q. Liu, H. E. Ruda, G. M. Chen, and M. Simard-Normandin, J. Appl. Phys. **79**, 7790 (1996).
- ³²L. Kronik and Y. Shapira, J. Vac. Sci. Technol. A **11**, 3081 (1993).
- ³³L. Kronik, L. Burstein, Y. Shapira, and M. Oron, Appl. Phys. Lett. **63**, 60 (1993).
- ³⁴Q. Liu, C. Chen, and H. Ruda, J. Appl. Phys. **74**, 7492 (1993).
- ³⁵L. Kipp, R. Adlung, N. Trares-Wrobel, and M. Skibowski, Appl. Phys. Lett. **74**, 1836 (1999).
- ³⁶S. Kumar, T. Ganguli, P. Bhattacharya, U. N. Roy, S. S. Chandvankar, and B. M. Arora, Appl. Phys. Lett. **72**, 3020 (1998).
- ³⁷M. Leibovitch, L. Kronik, E. Fefer, V. Korobov, and Y. Shapira, Appl. Phys. Lett. **66**, 457 (1995).
- ³⁸N. Bachrach-Ashkenasy, L. Kronik, Y. Shapira, Y. Rosenwaks, M. C. Hanna, M. Leibovitch, and P. Ram, Appl. Phys. Lett. **68**, 879 (1996).
- ³⁹N. Ashkenasy, M. Leibovitch, Y. Shapira, F. Pollak, G. T. Burnham, and X. Wang, J. Appl. Phys. **83**, 1146 (1998).
- ⁴⁰M. Leibovitch, L. Kronik, E. Fefer, L. Burstein, V. Korobov, and Y. Shapira, J. Appl. Phys. **79**, 8549 (1996).
- ⁴¹L. Aigouy, F. H. Pollak, J. Petruzzello, and K. Shahzad, Solid State Commun. **102**, 877 (1997).
- ⁴²B. Q. Sun, Z. D. Lu, D. S. Jiang, J. Q. Wu, Z. Y. Xu, Y. Q. Wang, J. N. Wang, and W. K. Ge, Appl. Phys. Lett. **73**, 2657 (1998).
- ⁴³L. Burnstein, Y. Shapira, J. Partee, J. Shinar, Y. Lubianiker, and I. Balberg, Phys. Rev. B **55**, R1930 (1997).
- ⁴⁴Lord Kelvin, Philos. Mag. **46**, 82 (1898); see, also, Ref. 5 for a detailed review of all experimental methods used in SPV measurements.
- ⁴⁵W. H. Brattain and J. Bardeen, Bell Syst. Tech. J. **32**, 1 (1953).
- ⁴⁶W. A. Zisman, Rev. Sci. Instrum. **3**, 367 (1932).
- ⁴⁷S. R. Morrison, J. Phys. Chem. **57**, 860 (1953).
- ⁴⁸C. Munakata, K. Yagi, T. Warabisako, M. Nanba, and S. Matsubara, Jpn. J. Appl. Phys. **21**, 624 (1982).
- ⁴⁹K. Kinameri, C. Munakata, and K. Mayama, J. Phys. E **21**, 91 (1988).
- ⁵⁰J. Hlavka and R. Svehla, Rev. Sci. Instrum. **67**, 2588 (1996).
- ⁵¹R. J. Phelan, Jr. and J. O. Dimmock, Appl. Phys. Lett. **10**, 55 (1967).
- ⁵²Y. Byun and B. W. Wessles, Appl. Phys. Lett. **52**, 1352 (1988).
- ⁵³E. M. Logothetis, H. Holloway, A. J. Varga, and E. Wilkes, Appl. Phys. Lett. **19**, 318 (1971).
- ⁵⁴L. J. Jastrzebski and J. Lagowski, RCA Rev. **41**, 188 (1980).
- ⁵⁵J. Lagowski, L. Jastrzebski, and G. W. Cullen, J. Electrochem. Soc. **128**, 2665 (1981).
- ⁵⁶F. Yan, X. M. Bao, and T. Gao, Solid State Commun. **91**, 341 (1994).
- ⁵⁷N. Mirowska and J. Misiewicz, Semicond. Sci. Technol. **7**, 1332 (1992).
- ⁵⁸B. Wang, D. Wang, Y. Cao, X. Chai, X. Geng, and T. Li, Thin Solid Films **284–285**, 588 (1996).
- ⁵⁹B. Wang, D. Wang, L. Zhang, and T. Li, J. Phys. Chem. Solids **58**, 25 (1997).
- ⁶⁰B. Wang, D. Wang, L. Zhang, and T. Li, Thin Solid Films **293**, 40 (1997).
- ⁶¹J. I. Pancove, *Optical Process in Semiconductors* (Dover, New Jersey, 1971), Chap. 14, p. 304. Also see, Y. Yan, Appl. Phys. Lett. **71**, 407 (1997).
- ⁶²B. O. Seraphin, R. B. Hess, and N. Bottka, J. Appl. Phys. **36**, 2242 (1965); see, also, Ref. 6, p. 470, for an expression of $\Delta\alpha$.
- ⁶³M. Cardona, in *Solid State Physics Supplement*, edited by F. Seitz, D. Turnbull, and H. Ehrenreich (Academic, New York, 1969), Vol. 11, p. 105.
- ⁶⁴D. E. Aspnes, in *Handbook of Semiconductors*, edited by M. Balakanski (North-Holland, New York, 1980), Vol. 2, p. 118, Table 1.
- ⁶⁵Y. P. Varshni, Physica **34**, 149 (1967).
- ⁶⁶R. Passler, J. Appl. Phys. **83**, 3356 (1998).
- ⁶⁷S. Datta, B. M. Arora, and S. Kumar, Phys. Rev. B **62**, 13 604 (2000).
- ⁶⁸E. Grilli, M. Guzzi, R. Zamboni, and L. Pavesi, Phys. Rev. B **45**, 1638 (1992).
- ⁶⁹S. Datta, M. Gokhale, A. P. Shah, B. M. Arora, and S. Kumar, Appl. Phys. Lett. (in press).